Using models to interpret the impact of roadside barriers on near-road air quality

Article *in* Atmospheric Environment · May 2016

DOI: 10.1016/j.atmosenv.2016.05.001

4 authors, including:

Nico Schulte
California Air Resources Board
11 PUBLICATIONS **29** CITATIONS
SEE PROFILE

Akula Venkatram
University of California, Riverside
166 PUBLICATIONS **2,812** CITATIONS
SEE PROFILE

Accepted Manuscript

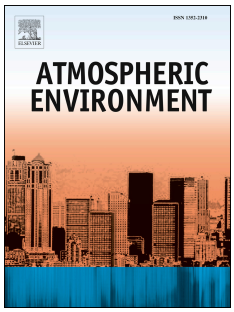

Using models to interpret the impact of roadside barriers on near-road air quality

Seyedmorteza Amini, Faraz Enayati Ahangar, Nico Schulte, Akula Venkatram

PII: S1352-2310(16)30333-8

DOI: 10.1016/j.atmosenv.2016.05.001

Reference: AEA 14587

To appear in: *Atmospheric Environment*

Received Date: 28 October 2015

Revised Date: 18 April 2016

Accepted Date: 2 May 2016

Please cite this article as: Amini, S., Ahangar, F.E., Schulte, N., Venkatram, A., Using models to interpret the impact of roadside barriers on near-road air quality, *Atmospheric Environment* (2016), doi: 10.1016/j.atmosenv.2016.05.001.

Using Models to Interpret the Impact of Roadside Barriers on Near-Road Air Quality

By

Seyedmorteza Amini, Faraz Enayati Ahangar, Nico Schulte and Akula Venkatram

University of California, Riverside, CA

Abstract

The question this paper addresses is whether semi-empirical dispersion models based on data from controlled wind tunnel and tracer experiments can describe data collected downwind of a sound barrier next to a real-world urban highway. Both models are based on the mixed wake model described in Schulte et al. (2014). The first neglects the effects of stability on dispersion, and the second accounts for reduced entrainment into the wake of the barrier under unstable conditions. The models were evaluated with data collected downwind of a kilometer-long barrier next to the I-215 freeway running next to the University of California campus in Riverside. The data included measurements of 1) ultrafine particle (UFP) concentrations at several distances from the barrier, 2) micrometeorological variables upwind and downwind of the barrier, and 3) traffic flow separated by automobiles and trucks. Because the emission factor for UFP is highly uncertain, we treated it as a model parameter whose value is obtained by fitting model estimates to observations of UFP concentrations measured at distances where the barrier impact is not dominant. Both models provide adequate descriptions of both the magnitude and the spatial variation of observed concentrations. The good performance of the models reinforces the conclusion from Schulte et al. (2014) that the presence of the barrier is equivalent to shifting the line sources on the road upwind by a distance of about HU/u_* where H is the barrier height, U is the wind velocity at half of the barrier height, and u_* is the friction velocity. The models predict that a 4 m barrier results in a 35% reduction in average concentration within 40 m (10 times the barrier height) of the barrier, relative to the no-barrier site. This concentration reduction is 55% if the barrier height is doubled.

Keywords

Roadside Barrier, Dispersion modeling, Line Source, Near-Road Air Quality

1. Introduction

The majority of the studies (Gallagher et al., 2015) conducted to date indicate that solid barriers placed next to roads have a mitigating effect on near-road air quality. The physics that governs this effect has been elucidated through several studies, such as the wind-tunnel study conducted by Heist et al. (2009). Through measurements of wind flow patterns and concentration distributions around a 1:150 scale model of a 6 lane divided highway with roadside barriers they showed that the mitigating impact of barriers is governed by two mechanisms: the plume from the road becomes elevated by being forced over the barrier, and vertical dispersion is enhanced by the turbulence created in the wake of the barrier. King et al. (2009) suggest that even a low wall (~ 1m) on the leeside of a road can shield pedestrians from exposure to pollutants swept upwind by the reverse flow induced by buildings on the windward side. This mechanism is not examined in this paper.

The results from the wind tunnel were confirmed in a tracer study conducted by Finn et al. (2010). They studied the effects of a barrier by releasing SF_6 from two identical 54 m long line sources. One source was located 6 m upwind of a 90 m long, 6 m high solid barrier and the other had no structures next to it. Tracer concentrations were measured simultaneously on identical sampling grids downwind of the sources. Six sonic anemometers measured flow around the barrier. Carefully controlled experiments showed that the barrier reduced downwind concentrations over a wide range of atmospheric stabilities.

Field studies conducted next to roadways confirm that barriers mitigate the impact of vehicle-related emissions. For example, Hagler et al. (2012) found that UFP concentrations at 10 m behind the 6 m barrier were about 50% less than those measured at this distance downwind of road sections without a barrier. Baldauf et al. (2008) found that CO and PM concentrations were reduced by 15% to 50% within 50 m of the 6 m barrier. The effect of the barrier persisted up to at least 20 times the barrier height in these studies, after which the concentration approached the value that would occur without a barrier.

The measurements from the wind tunnel and tracer experiments have been described with a variety of mechanistic models. Hagler et al. (2011) and Steffens et al. (2014) used computational fluid dynamics (CFD) models to produce adequate descriptions of the data from the wind tunnel (Heist et al., 2009). Bowker et al. (2007) used the Quick Urban & Industrial

Complex (QUIC) flow model coupled with a Lagrangian particle dispersion model to produce concentration patterns that were roughly consistent with observations from Baldauf et al. (2008).

Schulte et al. (2014) developed a semi-empirical dispersion model to describe data from the wind tunnel and the tracer studies. This model parameterizes the major features of the flow and dispersion effects induced by a barrier to avoid the computational burden of mechanistic CFD models, which have their own set of parameterizations. It is designed to be incorporated into routinely used models such as AERMOD (Cimorelli et al., 2005) or RLINE (Snyder et al., 2013). In this paper, we evaluate the model with field data collected next to a real world roadside barrier to answer the question: Can a model developed with data from controlled experiments conducted with well-characterized sources and meteorology be used to estimate the impact of a road-side barrier next to a multilane highway on which the magnitudes of the distributed sources are highly uncertain?

2. Field Study

2.1 Site description

The field study was conducted adjacent to CA-60, U.S. Interstate 215 (I-215) in Riverside, California. The highway has a barrier section located on the University of California, Riverside campus (Figure 1). The freeway has average traffic flow rate of 200,000 vehicles/day. The meteorological data collected from UC Riverside Meteorological Station, which is 1 km away from the barrier site, indicates a dominant wind from west/southwest during the daytime as shown in Figure 2. Thus, the wind blows close to perpendicular to the freeway during the daytime, which makes it convenient to study barrier effects during daytime unstable conditions. During the night, the wind blows from east, and the barrier is located upwind of the road.

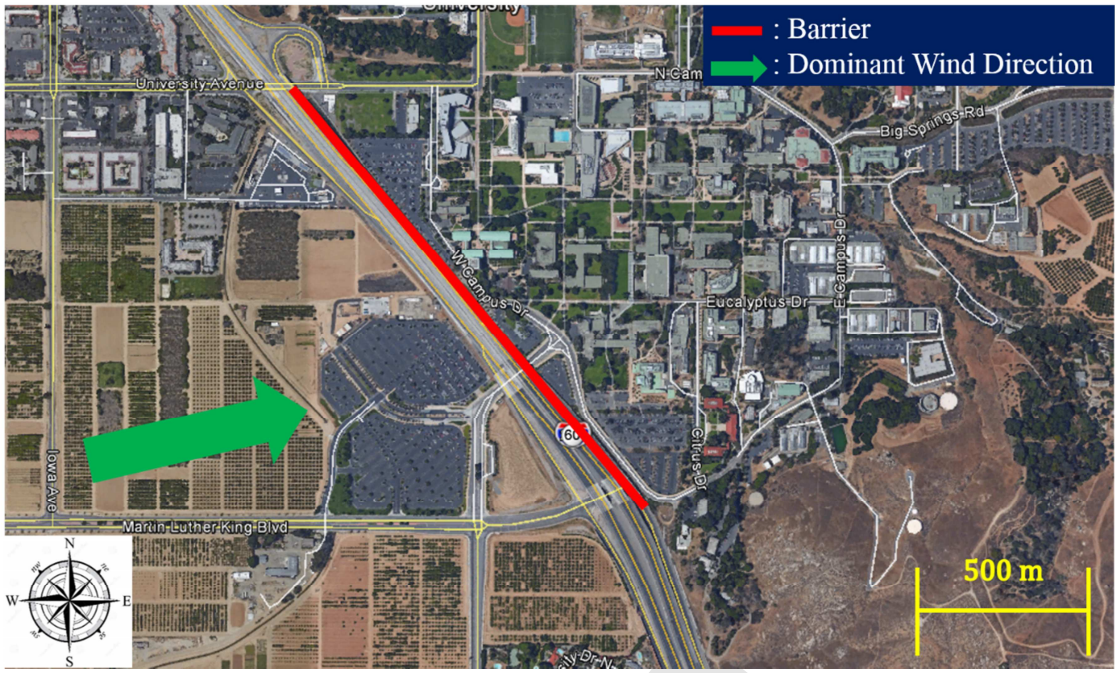

Figure 1- Map of the selected site. Adapted from Google Earth.

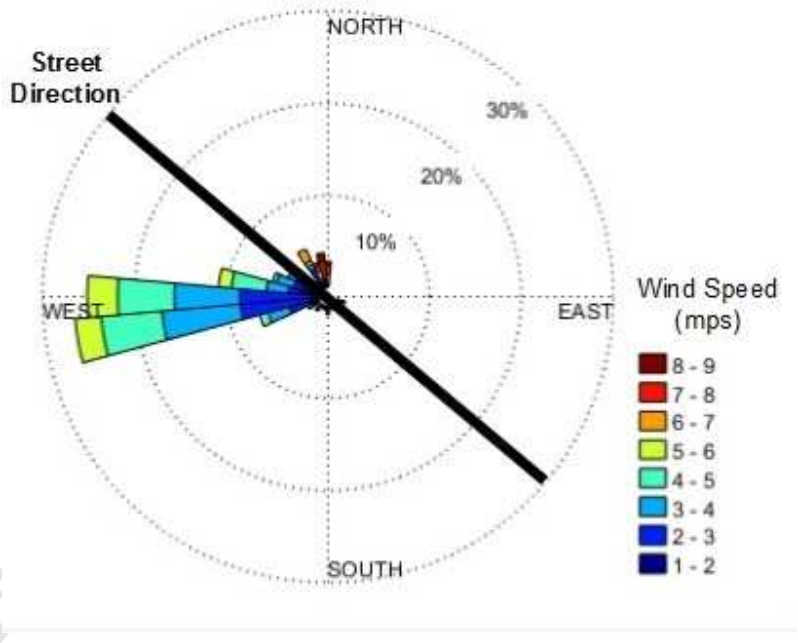

Figure 2- Wind rose from UC Riverside meteorological station and freeway direction at barrier site during February 2015.

The barrier, which is 3 m away from the edge of the road, is 4.5 m high and 1 km long. There are three lanes and one High Occupancy Vehicle (HOV) lane on the north bound side and

four lanes and one HOV lane on the south bound side of the freeway. There is an entrance to the north bound lanes and an exit on the south bound side of the freeway. The lanes are 3.5 m wide and the median is 10 m across. The freeway is at the same level as the adjacent streets. There is no major source of pollution within a 3.5 km radius of the barrier site except the freeway. The heading of the freeway is 140°. Therefore, the wind direction perpendicular to the freeway is 230° true to north. Two parking lots are located behind the barrier, which provide convenient locations for sampling.

The largest obstacles in the parking lots downwind of the barrier are widely scattered trees. There are no other major obstacles within 170 m of the barrier. A 2-lane street, West Campus Drive, runs parallel to the freeway between the parking lots. The street is mainly used to access the parking lots and the traffic is mainly passenger cars travelling during the morning hours, 8 A.M. to 10 A.M., and in the evening, 4 P.M. to 6 P.M. Another parking lot extends for 300 m west of the freeway. There is no major obstacle in this parking lot and trees are sparser and shorter than in the eastside parking lots.

2.2 Measurements

Ultrafine particles (UFPs) were used as the tracer in this study for several reasons. First, because they have adverse health effects, the levels of UFP concentrations next to a major highway are of public interest. Second, their concentrations next to major highways are well above background levels, and can be measured continuously with readily available instruments. Gidhagen et al. (2005) and Zhang et al. (2004) show that at the 100 m scale being considered here, deposition and coagulation play a minor role relative to turbulent dispersion in reducing particle number concentrations. Thus, UFP can be treated as a passive tracer by using particle number concentrations to characterize dispersion. One major problem with using UFP as a tracer is that UFP emission factors from vehicles are highly uncertain. Thus, it is necessary to treat the emission factor as an unknown whose value is obtained by fitting model estimates to measurements. This process is discussed in more detail in a later section.

Fifteen tests were conducted on different days and at different times of day from July 2014 to May 2015 but due to the malfunction of instruments and unfavorable meteorological conditions, only six tests were selected for analysis. Table 1 shows the dates and duration of measurements. The total duration of the 6 tests is 27 hours.

Table 1- Overview of dates and duration of measurements.

Test	UFP measurement dates	Time of Measurement
1	07/22/2014	12:00-17:00
2	08/11/2014	20:00-23:30
3	08/18/2014-08/19/2014	20:00-00:30
4	08/19/2014-08/20/2014	20:00-01:00
5	04/07/2015	12:30-17:00
6	05/05/2015	14:00-18:30

2.2.1 Air Quality Measurements

UFP number concentrations were measured using TSI Condensation Particle Counters (CPC), Model 3022A. The cutoff size of these CPCs is 7 nm. The measured concentration range was $5 \times 10^3 - 10^5$ particles/cm^3. According to the CPC manual, accuracy within this range of concentrations is $\pm 10\%$. The CPC concentrations were stored on a custom-designed data logger.

Several CPCs were used to measure background UFP concentrations and downwind UFP concentrations at several downwind distances. A CPC was placed at the upwind side of the freeway (assuming that the wind is blowing WSW) to measure background UFP number concentrations. The rest of the CPCs were deployed behind the barrier (Figure 3). The downwind CPCs were placed at least 250 m away from the barrier edge to avoid barrier edge effects. CPC locations were changed from one test to another to avoid any systematic bias in measurements. The background concentrations were subtracted from the downwind concentrations to estimate contributions from vehicles on the highway.

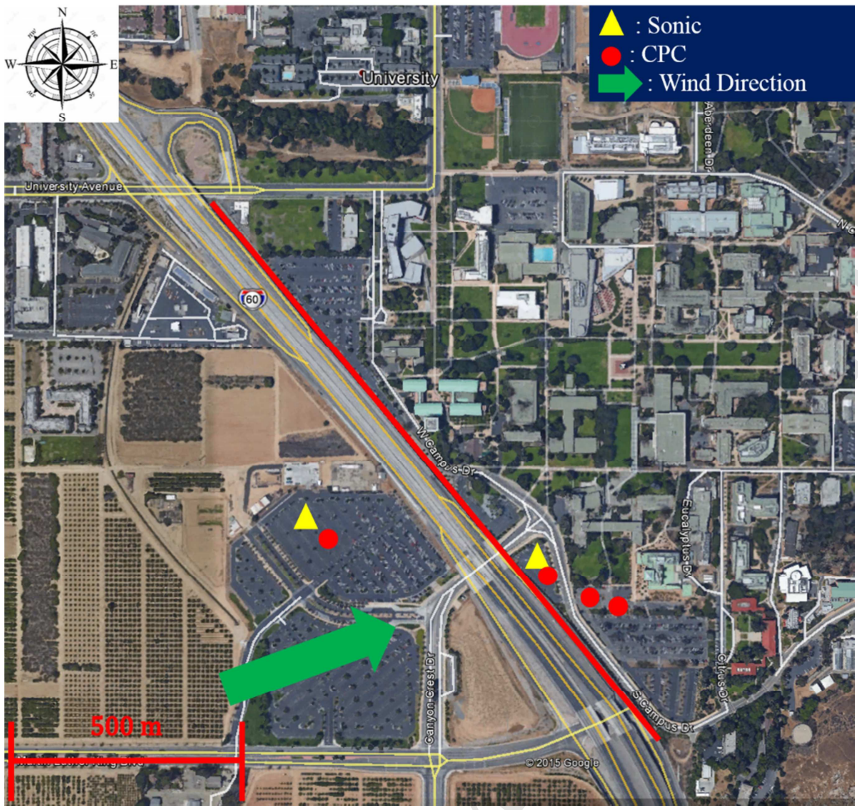

Figure 3- Approximate location of instruments.

2.2.2 Meteorology

Campbell Scientific CSAT3 3-D (three dimensional) Sonic Anemometers were used to measure flow properties. The measured data were stored on Campbell Scientific CR1000, CR3000, and CR5000 data loggers. Two 3-D sonic anemometers were employed to measure upwind and downwind flow characteristics. A sonic anemometer was attached to a light post on the upwind side of the freeway (parking lot 30; assuming wind is WSW) at 4 m height above ground level (AGL) to capture upwind flow characteristics. The UC Riverside Community Garden is located on the west side of the anemometer, which ensured the absence of any major obstacles to upwind wind flow. Another sonic anemometer was attached to a light post within the wake region behind the barrier at 4 m AGL to record flow characteristics behind the barrier.

2.2.3 Traffic Activity

The number of cars passing each lane of the freeway was downloaded from the CalTrans Performance Measurement System (www.pems.dot.ca.gov). The detectors record the number of cars and trucks separately.

3. Experimental Results

The wind direction during all the tests was within 45° of perpendicular to the freeway. The wind direction perpendicular to the freeway is 230° true to north. The meteorological conditions used to analyze the data correspond to the upwind 3-D sonic anemometer, which are shown in Table 2. The air quality data, micrometeorological data, and traffic data were averaged over 30-minute periods for analysis.

Table 2- Meteorological conditions.

Test	# of data points	Mean Monin-Obukhov Length (m)	Mean Wind Direction (deg true N)	Mean Wind Speed (ms^{-1})	Mean Friction Velocity (ms^{-1})	Cloud Cover
1	10	-11.5	254°	2.72	0.31	Clear
2	7	-15.7	256°	1.37	0.17	Clear
3	9	-9.1	238°	1.00	0.14	Clear
4	10	-5.8	254°	1.14	0.14	Clear
5	9	-38.8	238°	2.45	0.44	Mostly Cloudy
6	9	-43.0	268°	2.83	0.47	Partly Cloudy

Tests 1 through 4 were conducted in unstable conditions. Winds were moderate during test 1 and very light during tests 2, 3, and 4. No major variability in wind direction was observed during the first 4 tests and the wind directions were almost always favorable with respect to the freeway orientation. Skies were clear during the first 4 tests.

Notice that the surface boundary layer was unstable even during tests 2, 3, 4, which were conducted in the late evening and night when the sun had set. Tests 5 and 6 were conducted in near neutral conditions. Winds were moderate and the wind direction was steady. Wind directions were almost always favorable during these two tests. Skies were mostly cloudy in test 5 and partly cloudy in test 6.

The meteorological data measured by the UCR meteorological station (Figure 2) were consistent with the on-site sonic anemometer data, which indicated that the upwind anemometer was not affected by local obstacles.

The background concentrations were subtracted from the downwind concentrations in analyzing the UFP concentrations. The background concentration was around 10^4 #/cm^3. Figure 4 shows the spatial distributions of the averages over the concentrations measured in the six tests. The concentrations always decrease with distance behind the barrier and do not show the peak away from the barrier observed by Ning et al. (2010). We next examine whether these concentration measurements can be described with a dispersion model that was evaluated with data from controlled experiments conducted in the wind tunnel (Heist et al., 2009) and in the tracer field study (Finn et al., 2010).

a)

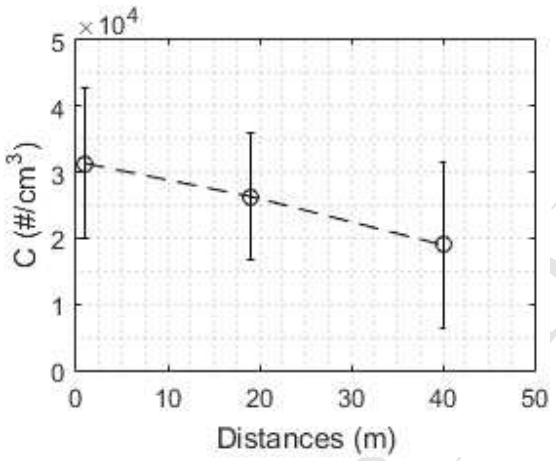

b)

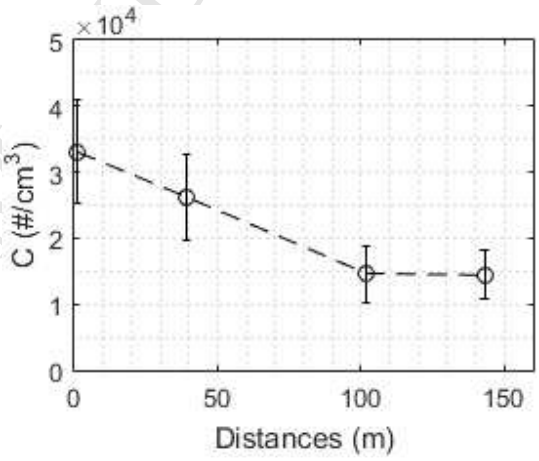

c)

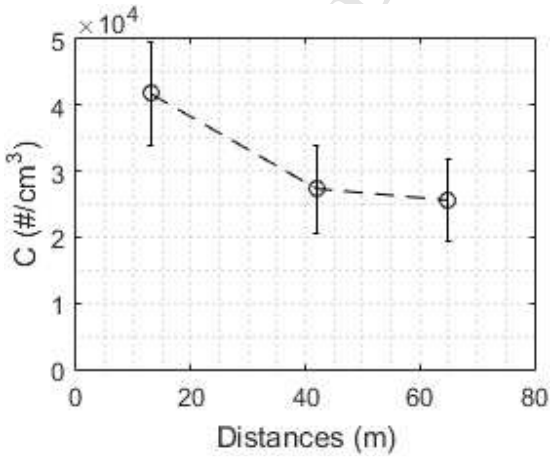

d)

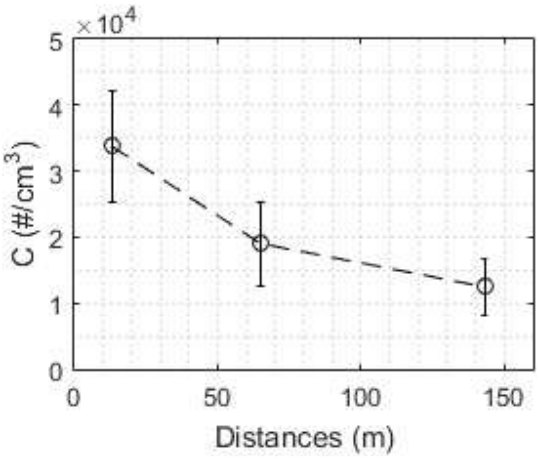

e)

f)

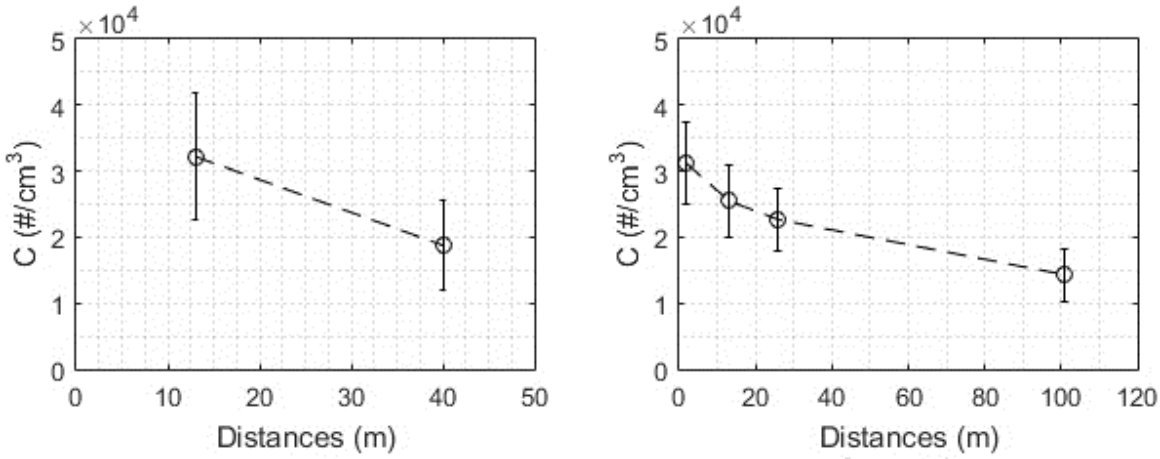

Figure 4- Averaged particle concentrations at different distances behind the barrier for a)Test 1, b)Test 2, c)Test 3, d)Test 4, e)Test 5, and f)Test 6.

4. Framework for the barrier models

The model (Schulte et al., 2014) used to interpret the data assumes that the concentration is well-mixed from the surface to the barrier height, and the concentration profile then follows a Gaussian distribution above the barrier height with the maximum concentration occurring at the barrier height, as shown in Figure 5. We can then express the surface concentration associated with an infinitely long line source as:

$$C_s = \frac{q}{U\left(\frac{H}{2}\right)\cos\theta\, H + U(\bar{z})\cos\theta\sqrt{\frac{\pi}{2}}\sigma_z} \quad (1)$$

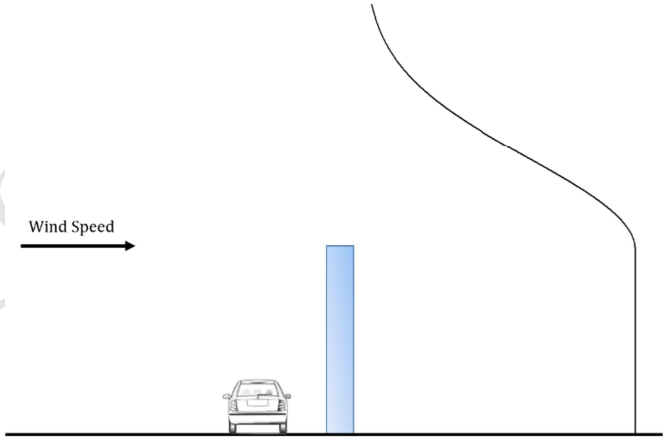

Figure 5- Schematic of concentration profile in Mixed-Wake model.

where q is the emission rate per length of the line source, C_s is the concentration at the surface, H is the barrier height, $U(\bar{z})$ is the wind speed at the effective centerline height of the plume above

the barrier, and θ is the wind direction with respect to the perpendicular to the road. The vertical plume spread, σ_z, is calculated using equations from Venkatram et al. (2013).

4.1 Simple barrier model

We can derive a simplified version of Equation 1 by using the neutral expression for the product of the effective wind speed and σ_z (Venkatram et al., 2013) :

$$U(\bar{z})\cos\theta\sqrt{\frac{\pi}{2}}\sigma_z = 0.57 * \sqrt{\frac{\pi}{2}}u_* x = 0.71u_* x \tag{2}$$

where u_* is the surface friction velocity and x is the distance of a receptor from the barrier. Equation 1 then becomes

$$C_s = \frac{q}{U\left(\frac{H}{2}\right)\cos\theta\, H + au_* x} \tag{3}$$

where a is 0.71.

Since the width of the road is comparable to the downwind distances being considered here, we treat the road as an area source with width *W*. Then, the concentration at a downwind distance *x* from the barrier becomes:

$$C_s = \int_x^{x+W} \frac{\frac{q}{W}}{U\left(\frac{H}{2}\right)\cos\theta\, H + au_* x}dx = \frac{q}{au_* W}\ln\left(1 + \frac{W}{H\frac{U\left(\frac{H}{2}\right)}{au_*}\cos\theta + x}\right) \tag{4}$$

This simple model, which applies primarily to neutral conditions, serves as a reference model whose performance against observations will be compared with that of a modified version.

4.2 Modified mixed-wake model

The second model considered here modifies Equation 1 to improve its performance during unstable conditions when Equation 1 overestimates concentrations close to the source in the Idaho Falls tracer experiment (Finn et al., 2010). The modified model assumes that the maximum concentration occurs above barrier height to be consistent with the wind tunnel data (Heist et al., 2009). The second modification is an entrainment factor, f_m, that reduces entrainment into the barrier wake during unstable conditions. This is an empirical modification to

account for the overestimation of concentrations close to the source under the unstable conditions of the Idaho Falls experiment. The factor reduces entrainment behind the barrier as the absolute value of the Monin-Obukhov length decreases. It is also a function of downwind distance, starting at values below unity just downwind of the barrier and approaches unity at large downwind distances. f_m is taken to be:

$$f_m = f_c + (1 - f_c)\left(1 - \exp\left(-\frac{x}{L_s}\right)\right) \tag{5}$$

where f_c, the entrainment factor at $x = 0$, is taken to be:

$$f_c = \exp\left(-\frac{L_s}{|L_{MO}|}\right) \tag{6}$$

where $L_s = 10H$ and H is the barrier height. f_c decreases as the absolute value of Monin-Obukhov length decreases.

The third modification is the effect of barrier on surface friction velocity. Surface friction velocity is enhanced based on an empirical model for the development of a neutral boundary layer after a roughness change,

$$u_{*w} = u_*\left(\frac{z_{0w}}{z_0}\right)^{0.17} \tag{7}$$

where the effective roughness of the wall is taken to be $z_{0w} = H/9$.

Assuming that the barrier does not modify the upwind heat flux, the Monin-Obukhov length is taken to be proportional to u_*^3. Then, the Monin-Obukhov length behind the barrier is:

$$L_w = L_{MO}\left(\frac{u_{*w}}{u_*}\right)^3 \tag{8}$$

The velocity below the barrier height is assumed to be uniform with height given by its value at $z = H$. With these parameterizations, the surface concentration can be expressed as

$$C_s = f_m C_{max}[\exp(-p_1^2) + \exp(-p_2^2)] \tag{9}$$

where C_{max} is the maximum concentration is

$$C_{max} = \frac{\frac{q}{\cos\theta}}{f_m U(H).H.[\exp(-p_1^2) + \exp(-p_2^2)] + U(\bar{z})\sqrt{\frac{\pi}{2}}\sigma_z.[2 - \mathrm{erf}(p_1) - \mathrm{erf}(p_2)]} \tag{10}$$

In this equation, $U(H)$ is the velocity at barrier height, $p_1 = (H - H_p)/\sqrt{2}\sigma_z$, $p_2 = (H + H_p)/\sqrt{2}\sigma_z$, and H_p is the height of maximum concentration, taken to be:

$$H_p = H + \frac{\sigma_{z_B}}{2} \quad (11)$$

where σ_{z_B} is the vertical plume spread right behind the barrier. This model performs better than the model presented in Schulte et al. (2014) in describing concentrations close to the barrier in the Idaho Falls experiment (Finn et al., 2010) during unstable conditions, which correspond to those considered in the current field study.

5. Comparison with observations

As indicated earlier, the UFP number emission factor is highly uncertain. The literature reports a large range 10^{12}~10^{14}#/(veh.km) (Kumar et al., 2011; Morawska et al., 2008). In this study, we treat the emission factor as an unknown parameter whose value is obtained by fitting model estimates to measured UFP concentrations. Because we wanted to evaluate the performance of the model in describing the impact of the barrier on downwind concentrations, we excluded data points at distances less than 40 m from the barrier in deriving the emission factor.

The ratio of UFP High Duty Vehicle (HDV) emission factor to that of Light Duty Vehicle (LDV) was taken to be 25. This ratio was found using $PM_{2.5}$ emissions from the EMFAC Model inventory data (California Air Resources Board, 2011). Car and truck emission factors were averaged over mileage for the fleet operating in Riverside County.

For the simple barrier model, the fitted emission factor is 7.90×10^{13} #/(veh.km) averaged over the six tests and a standard deviation of 2.88×10^{13} #/(veh.km). The corresponding statistics for the modified mixed-wake model are a mean of 7.09×10^{13} #/(veh.km) and a standard deviation of 2.56×10^{13} #/(veh.km). The mean emission factors of both models lie within the range reported in literature (Kumar et al., 2011; Morawska et al., 2008).

The performance of the models are evaluated using the geometric mean (m_g), standard deviation of the residuals between the observations and predictions (s_g), the fraction of data points that lie within a factor of two of the observations (fact2), and the correlation coefficient between the observations and predictions (r^2). The geometric mean and standard deviation are defined as:

$$\ln m_g = \sum_i \frac{\epsilon_i}{N} \tag{12}$$

$$\ln s_g = \sqrt{\frac{\sum_i \left(\epsilon_i - \ln m_g\right)^2}{N-1}} \tag{13}$$

where $\epsilon = \ln C_{obs.} - \ln C_{pred.}$ is the residual between the observed concentration and the predicted one, and N is the number of data points.

The performance of the models using the average emission factor for the six tests is shown in Figure 6. The r^2 are similar for the two models using a barrier height of 4.5 m.

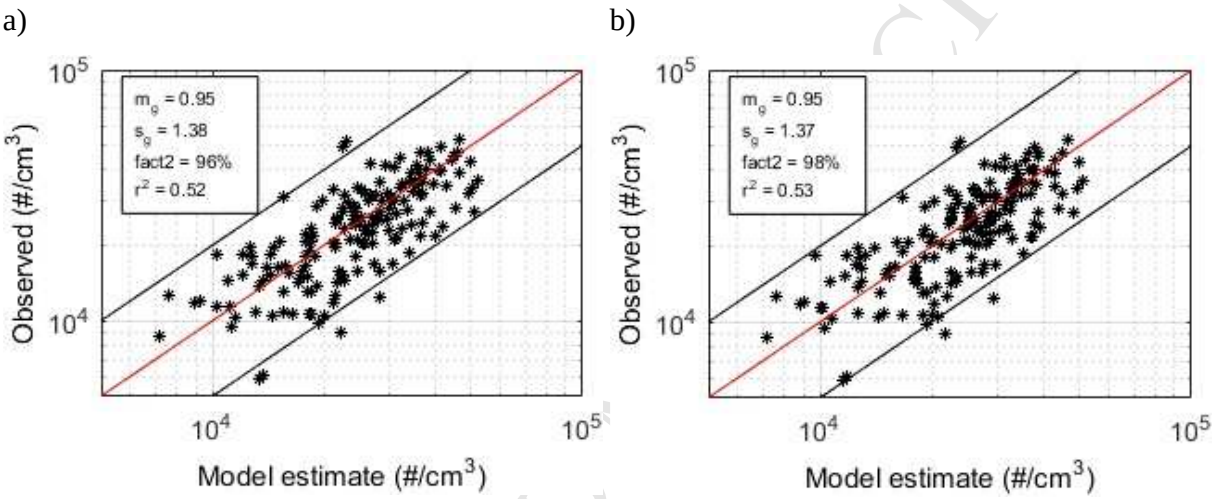

Figure 6- Comparison of observations and a) simple barrier model estimates and b) the modified mixed-wake model estimates.

To distinguish between the two models, we investigated the sensitivity of model performance to different barrier heights using fractional bias (Chang & Hanna, 2004) to measure their relative performance. Figure 7 shows the fractional bias versus barrier heights for both models. The bias is close to zero for both models when the barrier height is close to its actual value of 4.5 m, which indicates that both models capture the essential effects of barriers on downwind concentrations. The simpler barrier model is more sensitive to barrier height, reflecting the role of this variable in its formulation. It would be necessary to conduct experiments with varying barrier heights to check whether this sensitivity is real. .

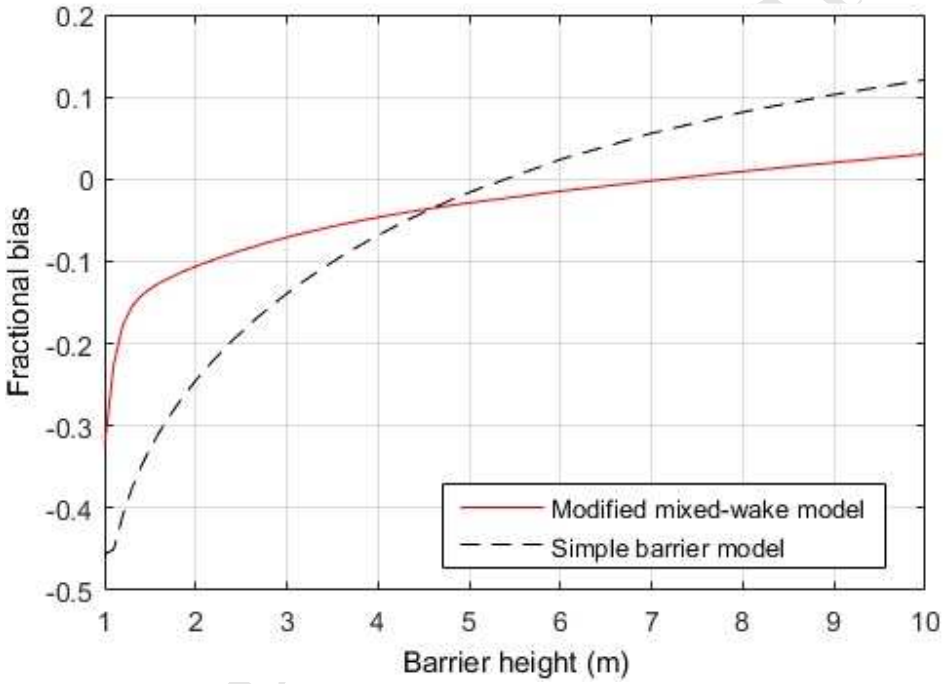

Figure 7- Fractional bias versus barrier height for modified mixed-wake model (red solid line) and for simple barrier model (black dashed line).

Figure 8, which compares measured concentration gradients with model estimates from test 3, the day with the lowest wind speed, test 4, the most convective day, and test 6, the most neutral day, indicates that both models provide a realistic depiction of the gradients over a wide range of stabilities.

1

a)

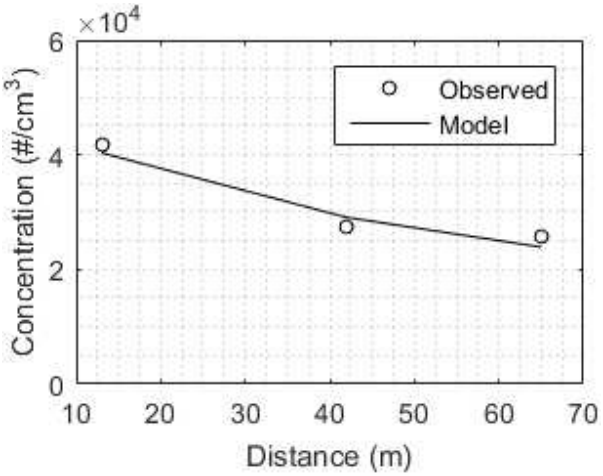
×10^4
Concentration (#/cm^3)
Distance (m)
Observed
Model

b)

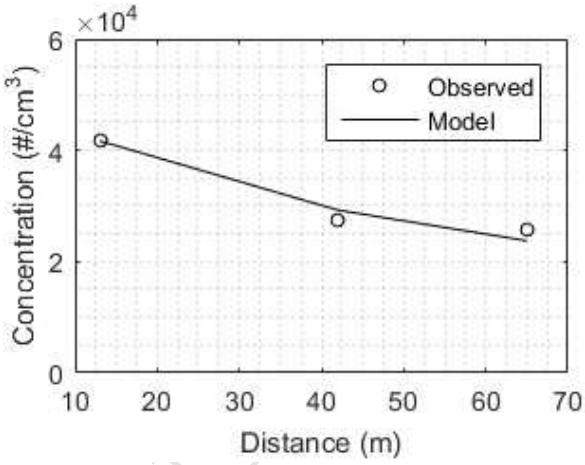
×10^4
Concentration (#/cm^3)
Distance (m)
Observed
Model

c)

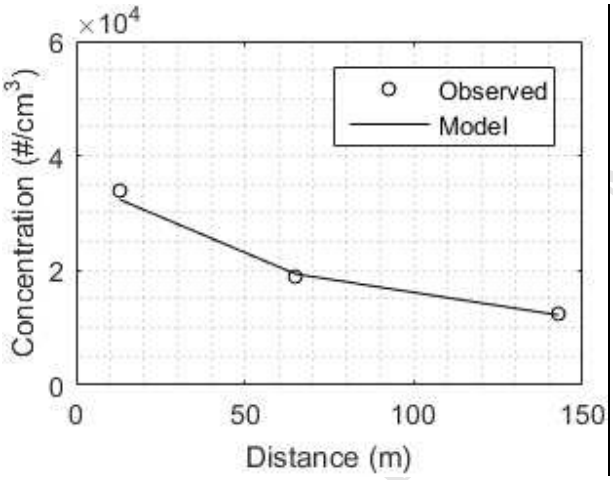
×10^4
Concentration (#/cm^3)
Distance (m)
Observed
Model

d)

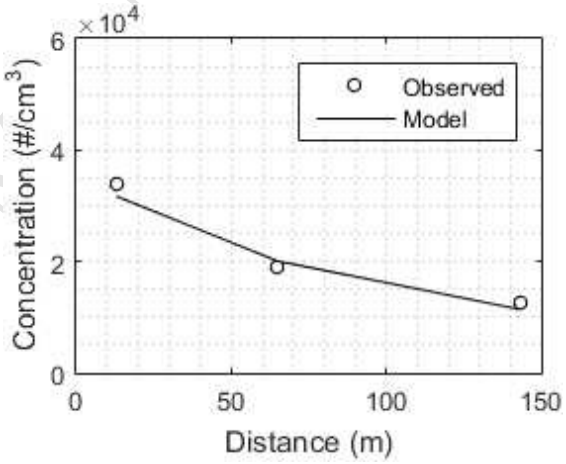
×10^4
Concentration (#/cm^3)
Distance (m)
Observed
Model

e)

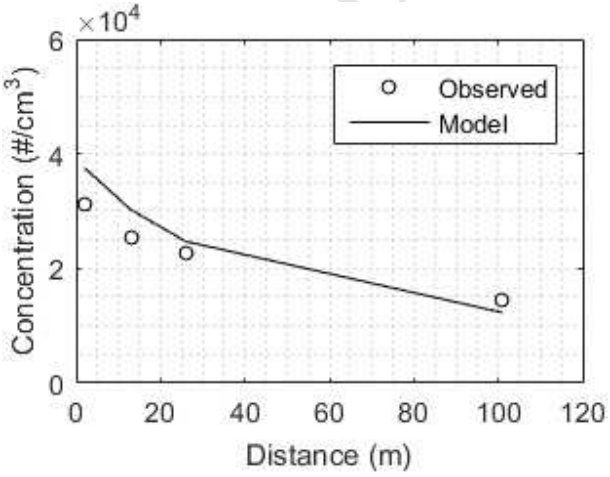
×10^4
Concentration (#/cm^3)
Distance (m)
Observed
Model

f)

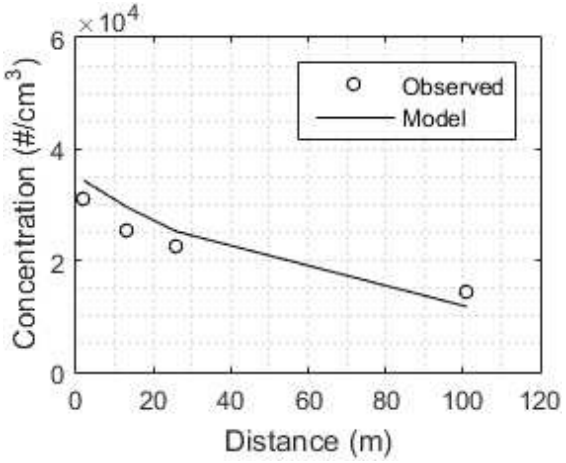
×10^4
Concentration (#/cm^3)
Distance (m)
Observed
Model

Figure 8- Concentration gradients for observations and a) simple barrier model for test 3, b) the modified mixed-wake model for test 3, c) simple barrier model for test 4, d) the modified mixed-wake model for test 4, e) simple barrier model for test 6, and f) the modified mixed-wake model for test 6. (Emission factors are calculated for each day using the data measured beyond 40 m from the barrier.)

Because the wind directions during all the tests were within **45**° perpendicular to the freeway, we cannot quantify the performance of the model when the wind direction is close to parallel to the road.

Figure 9 shows the spatial variation of the ratio of UFP concentrations in the presence of a barrier to those in the absence of the barrier as a function of barrier height; the micro-meteorological inputs correspond to test 6. In the simpler model, the no-barrier concentrations were estimated by treating the vehicles on the freeway as a 1 m barrier. The concentrations in modified mixed-wake model were estimated by assuming that the vehicles induce an initial vertical spread of 1 m. The concentration reduction, relative to the no-barrier concentration, just next to the 4 m barrier is 50-60%. This reduction increases to 65-75% by doubling the barrier height. The concentration reduction decreases with distance to about 25% at 40 m for the 4 m barrier. This reduction is 45% for the 8 m barrier. The average concentration reduction from 0-40 m is around 35% for a 4 m barrier. This average reduction increases to 55% with a doubling of the barrier height to 8 m.

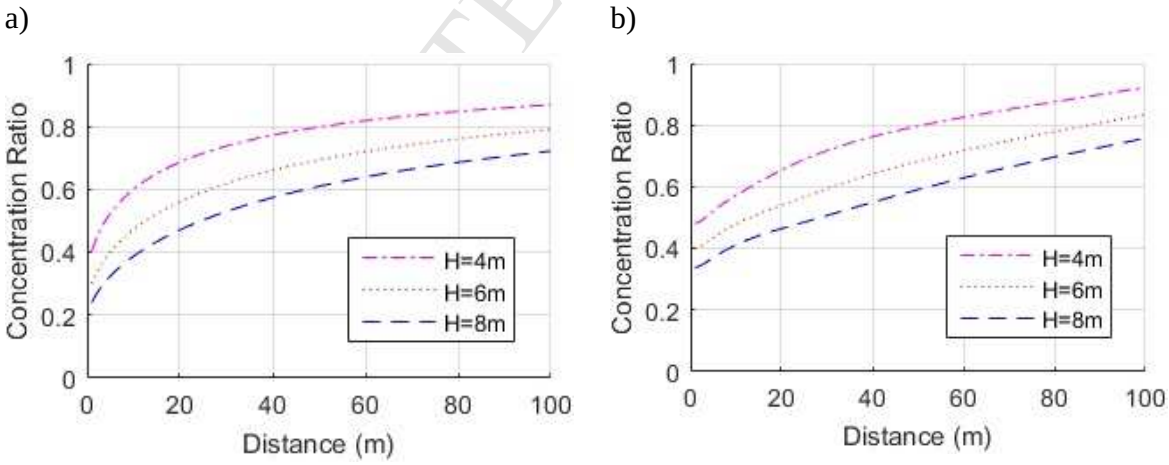

Figure 9- Comparison of estimated normalized concentrations, to no-barrier case, behind barriers with different heights for a) simple barrier model and b) the modified mixed-wake model.

6. Summary and Conclusions

We used data from a field study to evaluate a dispersion model that parameterizes the effects of roadside barriers on dispersion. This model was developed using data from experiments conducted in the wind tunnel and measurements from a tracer study in which concentrations were sampled simultaneously downwind from two line sources, one behind a 6 m barrier and the other located in open terrain. The primary question this paper addresses is whether a semi-empirical dispersion model based on data from controlled experiments can be used to interpret data collected downwind of a sound barrier next to a real-world urban highway with distributed sources whose magnitudes are uncertain.

Six tests were conducted next to a congested freeway, which had several factors that aided the interpretation of the data: 1) absence of a major source of pollution, except the freeway, in the neighborhood, 2) absence of a major obstacles on the east and west sides of the freeway, except the noise barrier, 3) absence of a busy street behind the barrier, 4) presence of a single barrier downwind of the freeway, and 5) presence of parking lots on both sides of the freeway to provide the opportunity to place several CPCs to measure UFP concentrations.

Two models were evaluated with the data from the field study. The first is a simplified version of model presented in Schulte et al. (2014), which assumes neutral conditions. The second is a modification of the model described in Schulte et al. (2014) to account for reduced entrainment in the immediate wake of the barrier during unstable conditions. Both models performed well in estimating the pollutant concentrations. Because the emission factor for UFP is highly uncertain, we treated it as a model parameter whose value was obtained by fitting model estimates to observations of UFP concentrations measured at distances where the barrier impact is small. The emission factors were found to have a mean of 7.90×10^{13} #/(veh.km) and a standard deviation of 2.88×10^{13} #/(veh.km) for the simple barrier model and a mean of 7.09×10^{13} #/(veh.km) and a standard deviation of 2.56×10^{13} #/(veh.km) for the modified mixed-wake model for all of the six tests. These values are well within the range reported in the literature (Kumar et al., 2011; Morawska et al., 2008).

Both models provide adequate estimates of the magnitudes and the spatial variation of near-road concentrations associated with vehicle-related emissions. The models were evaluated under unstable conditions when exposure to vehicle emissions is likely to be the highest for people living close to highways. Their applicability to stable conditions, when near-road

concentrations are relatively high, has not been evaluated. The models have also not been tested when the wind direction departs significantly from normal to the road.

The models predict that a 4 m barrier results in a 35% reduction in average concentration within 40 m (10 barrier heights) of the barrier, relative to the no-barrier site. This concentration reduction is 55% when the barrier height is doubled. The good performance of the simple barrier model reinforces the conclusion from Schulte et al. (2014) that the primary impact of the barrier is equivalent to shifting the line sources on the road upwind by a distance of about $HU/u_*cos\theta$.

Acknowledgements

The research reported in this paper was supported by the California Air Resources Board under contract number 13-306.

References

Baldauf, R., Thoma, E., Khlystov, a., Isakov, V., Bowker, G., Long, T., & Snow, R. (2008). Impacts of noise barriers on near-road air quality. *Atmospheric Environment*, *42*(32), 7502–7507. http://doi.org/10.1016/j.atmosenv.2008.05.051

Bowker, G. E., Baldauf, R., Isakov, V., Khlystov, A., & Petersen, W. (2007). The effects of roadside structures on the transport and dispersion of ultrafine particles from highways. *Atmospheric Environment*, *41*(37), 8128–8139. http://doi.org/10.1016/j.atmosenv.2007.06.064

California Air Resources Board, 2007. EMFAC2007 Users Guide. Mobile Source Emission Inventory. http://www.arb.ca.gov/msei/documentation.htm

Chang, J. C., & Hanna, S. R. (2004). Air quality model performance evaluation. *Meteorology and Atmospheric Physics*, *87*(1-3), 167–196.

Cimorelli, A. J., Perry, S. G., Venkatram, A., Weil, J. C., Paine, R. J., Wilson, R. B., … Brode, R. W. (2005). AERMOD: A Dispersion Model for Industrial Source Applications. Part I: General Model Formulation and Boundary Layer Characterization. *Journal of Applied Meteorology*, *44*(5), 682–693. http://doi.org/10.1175/JAM2227.1

Finn, D., Clawson, K. L., Carter, R. G., Rich, J. D., Eckman, R. M., Perry, S. G., … Heist, D. K. (2010). Tracer studies to characterize the effects of roadside noise barriers on near-road pollutant dispersion under varying atmospheric stability conditions. *Atmospheric Environment*, *44*(2), 204–214. http://doi.org/10.1016/j.atmosenv.2009.10.012

Gallagher, J., Baldauf, R., Fuller, C. H., Kumar, P., Gill, L. W., & McNabola, A. (2015). Passive methods for improving air quality in the built environment: A review of porous and solid

barriers. *Atmospheric Environment*, *120*, 61–70. http://doi.org/10.1016/j.atmosenv.2015.08.075

Gidhagen, L., Johansson, C., Langner, J., & Foltescu, V. L. (2005). Urban scale modeling of particle number concentration in Stockholm. *Atmospheric Environment*, *39*(9), 1711–1725. http://doi.org/10.1016/j.atmosenv.2004.11.042

Hagler, G. S. W., Lin, M. Y., Khlystov, A., Baldauf, R. W., Isakov, V., Faircloth, J., & Jackson, L. E. (2012). Field investigation of roadside vegetative and structural barrier impact on near-road ultrafine particle concentrations under a variety of wind conditions. *Science of the Total Environment*, *419*, 7–15. http://doi.org/10.1016/j.scitotenv.2011.12.002

Hagler, G. S. W., Tang, W., Freeman, M. J., Heist, D. K., Perry, S. G., & Vette, A. F. (2011). Model evaluation of roadside barrier impact on near-road air pollution. *Atmospheric Environment*, *45*(15), 2522–2530. http://doi.org/10.1016/j.atmosenv.2011.02.030

Heist, D. K., Perry, S. G., & Brixey, L. a. (2009). A wind tunnel study of the effect of roadway configurations on the dispersion of traffic-related pollution. *Atmospheric Environment*, *43*(32), 5101–5111. http://doi.org/10.1016/j.atmosenv.2009.06.034

King, E. a., Murphy, E., & McNabola, a. (2009). Reducing pedestrian exposure to environmental pollutants: A combined noise exposure and air quality analysis approach. *Transportation Research Part D: Transport and Environment*, *14*(5), 309–316. http://doi.org/10.1016/j.trd.2009.03.005

Kumar, P., Ketzel, M., Vardoulakis, S., Pirjola, L., & Britter, R. (2011). Dynamics and dispersion modelling of nanoparticles from road traffic in the urban atmospheric environment-A review. *Journal of Aerosol Science*, *42*(9), 580–603. http://doi.org/10.1016/j.jaerosci.2011.06.001

Morawska, L., Ristovski, Z., Jayaratne, E. R., Keogh, D. U., & Ling, X. (2008). Ambient nano and ultrafine particles from motor vehicle emissions: Characteristics, ambient processing and implications on human exposure. *Atmospheric Environment*.

Ning, Z., Hudda, N., Daher, N., Kam, W., Herner, J., Kozawa, K., … Sioutas, C. (2010). Impact of roadside noise barriers on particle size distributions and pollutants concentrations near freeways. *Atmospheric Environment*, *44*(26), 3118–3127. http://doi.org/10.1016/j.atmosenv.2010.05.033

Schulte, N., Snyder, M., Isakov, V., Heist, D., & Venkatram, A. (2014). Effects of solid barriers on dispersion of roadway emissions. *Atmospheric Environment*, *97*, 286–295. http://doi.org/10.1016/j.atmosenv.2014.08.026

Snyder, M. G., Venkatram, A., Heist, D. K., Perry, S. G., Petersen, W. B., & Isakov, V. (2013). RLINE: A line source dispersion model for near-surface releases. *Atmospheric Environment*, *77*, 748–756. http://doi.org/10.1016/j.atmosenv.2013.05.074

1 Steffens, J. T., Heist, D. K., Perry, S. G., Isakov, V., Baldauf, R. W., & Zhang, K. M. (2014).
2 Effects of roadway configurations on near-road air quality and the implications on roadway
3 designs. *Atmospheric Environment*, *94*, 74–85.
4 http://doi.org/10.1016/j.atmosenv.2014.05.015

5 Venkatram, A., Snyder, M. G., Heist, D. K., Perry, S. G., Petersen, W. B., & Isakov, V. (2013).
6 Re-formulation of plume spread for near-surface dispersion. *Atmospheric Environment*, *77*,
7 846–855. http://doi.org/10.1016/j.atmosenv.2013.05.073

8 Zhang, K. M., & Wexler, A. S. (2004). Evolution of particle number distribution near
9 roadways—Part I: analysis of aerosol dynamics and its implications for engine emission
10 measurement. *Atmospheric Environment*, *38*(38), 6643–6653.
11 http://doi.org/10.1016/j.atmosenv.2004.06.043

12

- Roadside barriers produce effective mitigation of the impact of emissions
- Real-world barrier effects can be described with simple model
- Roadside barrier effects are equivalent to shifting source upwind
- Model can be used to design roadside barriers
- Model can be used to estimate UFP emission factors